

國立交通大學

電子工程學系電子研究所碩士班

碩 士 論 文

掃描鏈重新排列減少掃描移動功率

架構在非指定的測試集合



**Scan-Chain Reordering for Minimizing
Scan-Shift Power
Based on Non-Specified Test Cubes**

研 究 生：吳育澤

指 導 教 授：趙家佐 博士

中 華 民 國 九 十 七 年 一 月

掃描鏈重新排列減少掃描移動功率架構在非指定的測試集合

**Scan-Chain Reordering for Minimizing Scan-Shift Power Based on
Non-Specified Test Cubes**

研究生：吳育澤

Student : Yu-Ze Wu

指導教授：趙家佐

Advisor : Chia-Tso Chao

國立交通大學

電子工程學系電子研究所碩士班



A Thesis

Submitted to Department of Electronics Engineering & Institute of Electronics
College of Electrical and Computer Engineering
National Chiao Tung University
in Partial Fulfillment of the Requirements
for the Degree of
Master
in
Electronics Engineering
January 2008
Hsinchu, Taiwan, Republic of China
中華民國 九十七年一月

掃描鏈重新排列減少掃描移動功率架構在非指定的測試集合

學生：吳育澤

指導教授：趙家佐 博士

國立交通大學電子工程學系電子研究所碩士班

摘 要

這篇論文提出掃描元件的重新排列架構在非指定的測試集合，能保留測試圖案中不在乎位元的值用來減少在測試模式下所產生的信號變動量。首先，我們提出以掃描元件反應值之間的關係性來引導重新排列，並且用填值技術來減少掃描進的信號變動。接下來我們提出同時考慮掃描元件反應值和測試圖案之間的關係性來幫助排列並且同時減少掃描進和出的信號變動。一個反向的技術應用在此方法上進一步減少測試功率。除了功率導向的重新排列技術，我們最後提出同時考慮功率和繞線的方法，在兩者間做取捨以達到減少違背時間限制的情況發生。最後，我們做一些實驗來論證提出方法的有效性和優勢關於在減少掃描移動時所產生的信號變動。此外，關於同時考慮功率和繞線的情況也透過實驗來做討論。

**Scan-Chain Reordering for Minimizing Scan-Shift Power Based on
Non-Specified Test Cubes**

Student : Yu-Ze Wu

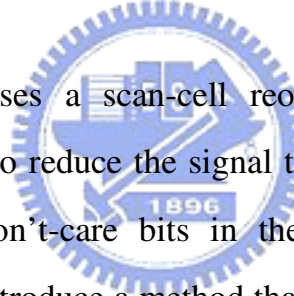
Advisor : Dr. Chia-Tso Chao

Department of electronics Engineering

Institute of Electronics

National Chiao Tung University

Abstract

The logo of National Chiao Tung University is a circular emblem with a gear-like border. Inside the circle, there is a stylized building and a banner with the year '1896'.

This thesis proposes a scan-cell reordering scheme based on unspecified test vectors to reduce the signal transitions during test mode while preserving the don't-care bits in the test patterns for a later optimization. First, we introduce a method that uses response correlations to guide the scan cell reordering and specify don't care bits through a pattern-filling technique to reduce scan-in transitions. Next, a proposed scheme utilizes both response correlation and pattern correlation to simultaneously minimize scan-out and scan-in transitions. An extension of the scheme that reverse-combined technique applied to the method further reduces test power. Except power-driven scan cell reordering methodology, we last propose a methodology that takes the routing overhead into consideration and derive a new ordering methodology based on power and routing concerns. We can make a tradeoff between power and routing to reduce timing violations. A series of experiments

demonstrate the effectiveness and superiority of the proposed scheme on reducing total scan-shift transitions. The effectiveness of the scheme considering both power and routing overhead is discussed through experiments as well.



誌 謝

時間過的很快，在交大兩年半的時間轉眼間就過去了。在這些日子中，雖然有遇到一些挫折，但很高興我有一群支持我、幫助我的人，讓我有可以去克服所遇到的困難。首先，我要感謝我的家人，在我遇到挫折的時候，他們總是給我鼓勵和支持，讓我在研究的旅途中可以無後顧之憂的走下去。另外，也非常感謝我的指導老師 趙家佐教授在研究過程中的指點迷津，每當我遇到瓶頸時，它總能給我些建議，好讓我的研究之路能更順利。在日常生活方面，老師也會有透過聊天的方式談些個人經歷來給於諄諄教誨，人生規劃上也有一些建議。

另外，也感謝實驗室的學弟啟銘、智為、偉勝在生活和研究上的交流。每當有程式方面的問題，偉勝總能給我蠻大的幫助，智為在工作站和 Tool 使用上的幫助，還有和啟銘討論研究方面的想法，這些都讓我在研究之路上更順遂。

最後，我要感謝我的朋友們、勇全、育農、昭銘、子宗、聖偉、伯翰、亦琦、俊宇、宗翰等一些曾在研究所生涯中陪伴過我的朋友，有了你們，才讓我的研究所生活更多采多姿、更加順利。最後，再次向所有曾支持、關懷、幫助我的人，沒有你們就沒有現在的我。

2008 年 吳育澤 撰

Contents

摘 要.....	i
Abstract	ii
誌 謝.....	iv
Contents.....	v
List of Tables.....	vii
List of Figures	viii
Chapter 1 Introduction	1
Chapter 2 Preliminaries	4
2.1 Scan-based Design.....	4
2.2 Test Power Challenge	6
Chapter 3 Power-driven Scan Cell Reordering	9
3.1 Previous Work.....	9
3.2 Motivation	12
3.3 Problem Formulation.....	14
3.4 Scan-cell Reordering Considering Only Response Correlation.....	16
3.4.1 Detailed Steps of Reordering Scheme.....	16
3.4.2 Experimental Results	20
3.5 Scan-cell Reordering Considering Both Response and Pattern Correlations	24
3.5.1 Detailed Steps of Reordering Scheme.....	24
3.5.2 Experimental Results	27
3.6 Scan-Cell Reordering Using Scan-data Inversion.....	29
3.6.1 Detailed Steps of Reordering Scheme.....	29
3.6.2 Experimental Results	35
Chapter 4 Scan Cell Reordering Considering Both Power and Routing Factors	37
4.1 Detail Steps of Reordering Considering both Power and Routing Overhead	37
4.1.1 Construct a Directed Multiple-Weight Graph Based on Correlations and Routing Overhead	38

4.1.2 Find the Hamiltonian path with the minimum WTC.....	38
4.1.3 Experimental Results	41
Chapter 5 Conclusions	44
References	45



List of Tables

Table 3-1 Response correlation of ISCAS benchmark s38584.	14
Table 3-2 Statistics of the circuits and their ATPG patterns	22
Table 3-3 Comparisons of generated scan-shift transitions between RORC and [20]	23
Table 3-4 Different cases of pattern correlations between two adjacent cells.	25
Table 3-5 Comparisons of generated scan-shift transitions between RORC and ROBPR.....	30
Table 3-6 Different cases of inverse pattern correlations between two adjacent cells.....	32
Table 3-7 Comparisons of generated scan-shift transitions between ROBPR and SIRO	36
Table 4-1 Comparisons of scan-shift transitions on different optimization factor value and tool ordering [27]	41
Table 4-2 Comparisons of scan chain length (um) on different optimization factor value and tool ordering [27]	42



List of Figures

Figure 2-1 A scan design schematic	5
Figure 2-2 An example of scan-in, capture, and scan-out operation.	6
Figure 3-1 Graph construction based on deterministic sets.....	10
Figure 3-2 Different transition weight for test vectors and responses.....	11
Figure 3-3 Identifying the input and output of scan chain	12
Figure 3-4 Calculation of scan-in and scan-out WTC	17
Figure 3-5 Main steps of the proposed reordering scheme RORC.....	18
Figure 3-6 Construction of a response-correlation graph.....	19
Figure 3-7 Estimated WTC_{out} of different scan-chain input/output.....	21
Figure 3-8 Main steps of the proposed reordering scheme ROBPR	24
Figure 3-9 Construction of the directed graph based on pattern and response correlations.....	26
Figure 3-10 The proposed algorithm for finding a Hamiltonian path with minimal WTC_{total}	28
Figure 3-11 Main steps of the proposed reordering scheme SIRO	31
Figure 3-12 Construction of the directed graph based on inverse and non-inverse correlation sets	33
Figure 3-13 Derive scan-in patterns in SIRO	34
Figure 3-14 Implement inverse techniques with traditional scan-chain architecture	35
Figure 4-1 Construction of the directed graph based on correlations and routing effects.....	39
Figure 4-2 The proposed algorithm for finding a Hamiltonian path optimizing power and routing overhead.....	40
Figure 4.3: The trends of transitions and chain length on different constrain factor and tool ordering	43

Chapter 1

Introduction

The scan design has been a widely used DFT technique which can guarantee high fault coverage for a complex design by enhancing its controllability and observability [1]. When using the scan design to shift test data, however, a large number of signal transitions may occur along the scan paths, which induces even more signal transitions on the circuit-under-test (CUT). Therefore, with the scan design, the CUT will consume much more power in its test mode than that in its functional mode [2]. This excessive power consumption during the scan-based testing may result in physical damage or reliability degradation to the CUT, and in turn decreases the yield and product lifetime [3]. Another concern of this increased power is that significant IR Drop [4] causes good chips classified as fails and thus reduces the yield. As the number of scan cells keeps on growing in modern designs, this increasing power consumption has become one of the biggest barriers to effective the scan-based testing.

A common practice to lower the power consumption during scan-based testing is to reduce the number of scan cell's signal transitions, which can be classified into the following three types: (1) the capture transition – generated by the same scan cell's value difference between the scan-in pattern and the corresponding captured response, (2) the scan-out transition – generated by two adjacent scan cells' value difference between their

scan-out response, and (3) the scan-in transition – generated by two adjacent scan cells' value difference between the scan-in patterns. The first transition type is associated with the capture power and the last two types are associated with the scan-shift power.

In order to reduce the capture transitions, complex ATPGs [5][6][7][8][9] are proposed to generate test-pattern vectors which have a minimal hamming distance with their corresponding test-response vectors. Because the don't care bits in their test cubes are fully specified for minimizing the capture transitions, the above ATPGs preclude the possibility for further test compaction or compression, and hence may result in a larger test set.

Methods are proposed to utilize the don't-care bits to minimize the scan-in transitions for a given test set [10][11][12][13]. [10] proposed a don't-care-filling technique, named MT-fill, guaranteeing that the scan-in transitions generated by its filled patterns are minimized for the given test set. The methods in [11][12] reduced the test power as well as the test data volume based on build-in de-compression hardware. [13] added Xor gates or inverters along the scan paths to minimize the scan-in transitions. However, none of [10][11][12][13] considered the scan-out transitions simultaneously.

Another concept to reduce the scan-shift power is to partition the scan cells into multiple groups and activate only one group at a time during the scan-shift cycles [14][15][16][17][18][19]. It can limit the concurrent transitions in a small portion of the CUT. The partition methods require special control architectures to the scan designs, such as gated clocks [14], central control unit for each group's clock signal [15][16], or specialized scan cells along with multiphase generator [18]. [19] further minimizes the capture power by only capturing responses for certain selected groups of scan cells. It requires a customized ATPG and discards a significant portion of responses.

Methods in [20][21] change the order of scan cells along the scan paths to minimize both scan-in and scan-out transitions based on given test patterns and responses. This scan-cell-reordering technique saves the scan-shift power, but sacrifices the opportunity

of optimizing the wire length of scan paths during the APR stage [22][23]. In [24][25], re-ordering concerning the power and wire length is proposed. The method is to minimize power as possible without violating the user-specific constraint of wire length. However, the existing scan-chain-reordering techniques [20][21][24][25] need to obtain the exact test patterns and responses in advance. As the result, no don't-care bits can be utilized for a further reduction to scan-in transitions or test data volume, such as [10][11][12][13].

In this thesis, we attempt to develop a scan-cell-reordering scheme which can minimize the scan-out transitions while preserving the don't-care bits in the test cubes for a later optimization of scan-in transitions using MT-fill [10]. To achieve this goal, we first need to predict the correlation between the response values before specifying don't-care bits. This response correlation is an index to the possible scan-out transitions between scan cells and can be used as a guidance to the reordering process. Next, we consider the impact of scan-cell reordering on the result of MT-fill and simultaneously optimize the scan-in and scan-out transitions. Last, a scan-cell reordering considering power and routing factors is presented. We take scan chain length into consideration and trade off between power and routing length by user-specific coefficient of cost function consisting of power and routing factors. The experimental results demonstrate the effectiveness and the superiority of the proposed reordering scheme over a previous scan-cell reordering scheme [20].

Chapter 2

Preliminaries

2.1 Scan-based Design

To reduce the testing cost, we focus in *design-for-test* (DFT) techniques that aim at improving the testability. There are difficulties with the use of ad-hoc DFT methods. First, circuits are too large for manual inspection. Second, human testability experts are often hard to find, while the algorithmically generated testability measures are approximate and do not always point to the source of the testability problem. Finally, even after DFT modifications are made, tests must be produced to enhance the fault coverage. Due to these reasons, the use of ad-hoc DFT is usually discouraged for larger circuits.

As the size and complexity of digital system grew, an alternative form of DFT, known as structured DFT. In structured DFT, extra logic and signals are added to the circuit so as to allow the test according to some predefined procedure. Apart from the normal functional mode, such a design will have one or more test modes. Commonly used structured methods are scan and built-in self test.

The main idea in *scan design* is to obtain control and observability for flips-flops. This is done by adding a test mode to the circuit such that when the circuit in this mode,

all flip-flops functionally form one or more shift registers. The inputs and outputs of these shift registers (also known as scan registers) are made into primary inputs (PIs) and primary outputs (POs). Thus, using the test mode, all flip-flops can be set to any desired states by shifting those logic states into the shift register. Similarly, the states of flip-flops are observed by shifting the contents of the scan register out. All flip-flops can be set or observed in a time that equals the number of flip-flops in the longest scan register. Figure 2.1 shows a complete scan design schematic.

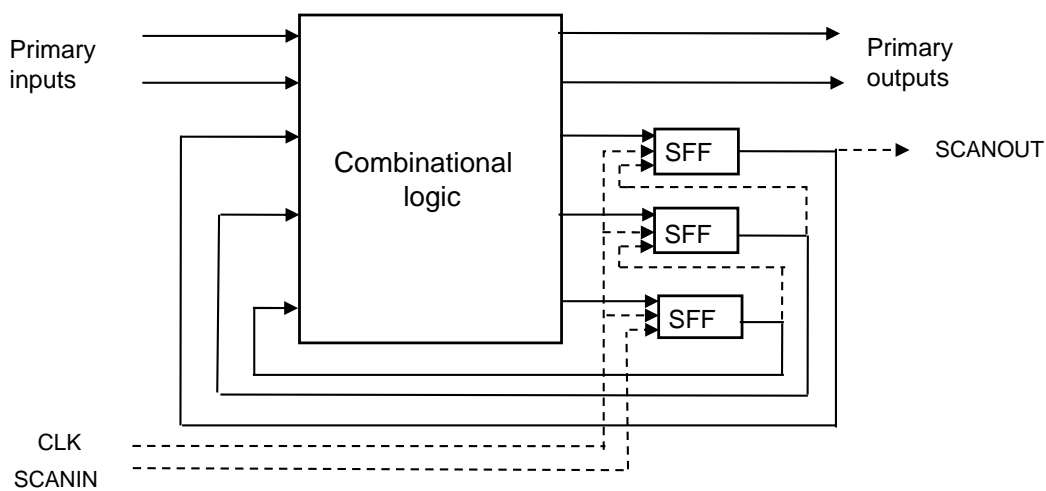


Figure 2.1: A scan design schematic.

Generally, the test mode of scan-based design consist of three operation : *scan-in operation*, *capture operation*, *scan-out operation*. During testing, the scan-based design first has to specify flip-flop cells with the pattern values obtained from *automatic test pattern generation* (ATPG) process. Next, the design executes one-cycle logic simulation to update flip-flop values in capture operation. Last, a serious of flip-flops response values is shifted out to be analyzed during scan-out operation. The scan-in and scan-out operation take several cycles which depend on the number of flips-flops of a scan-chain, but the capture operation takes one cycle.

Figure 2.2 illustrates the scan-in, capture, and scan-out operation. In the figure,

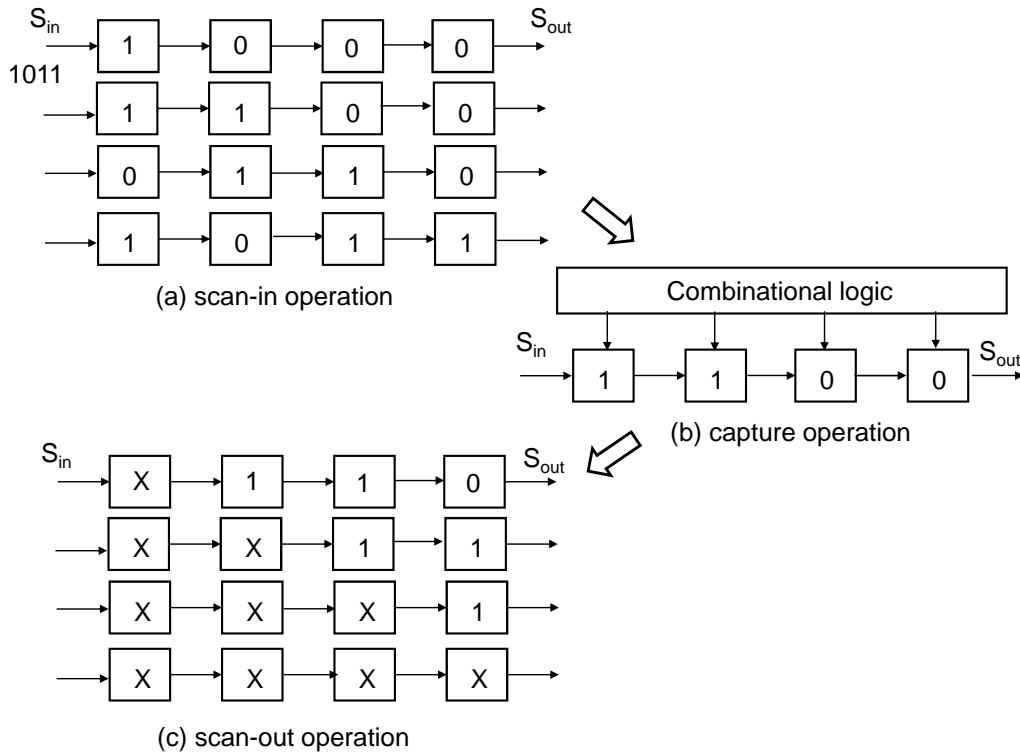


Figure 2.2: An example of scan-in, capture, and scan-out operation.

a four flip-flops scan chain (initialized cell values equal to 0) and a test vector 1011 is given. During scan-in operation, it take four cycles to shift in the vector values to scan cells, and then new cell values are loaded from combinational logic in capture cycle. Last, responses are scan-out while the next pattern is shifted in simultaneously (X s denote the values of next pattern) .

2.2 Test Power Challenge

Test power is a possible major engineering problem in the future of *system-on-chip* (SOC) development. As both the SoC designs and the deep-submicron geometry become prevalent, larger designs, tighter timing constrains, higher operating frequencies,

and lower applied voltages all affect the power consumption systems of silicon devices. More precisely, these factors affect energy, average power, instantaneous power, and peak power, so some characteristics are defined.

- **Energy:** The total switching activity generated during test application, energy affects the battery lifetime during power up or periodic self-test of battery-operated devices.
- **Average power:** Average power is the total distribution of power over a time period. The ratio of energy to test time gives the average power. Elevated average power increases the thermal load that must be vented away from the device under test to prevent structural damage (hot spots) to the silicon, bonding wires, or packages.
- **Instantaneous power:** Instantaneous power is the value of power consumed at any given instant. Usually, it is defined as the power consumed right after the application of a synchronizing clock signal. Elevated instantaneous power might overload the power distribution systems of the silicon or package, causing brown-out.
- **Peak power:** The highest power value at any given instant, peak power determines the component's thermal and electrical limits and system packaging requirements. If peak power exceeds a certain limit, designers can no longer guarantee that entire circuit will function correctly. In fact, the time window for defining peak power is related to the chip's thermal capacity, and forcing this window to one clock period is sometimes just a simplifying assumption. For example, consider a circuit that has a peak power consumption during only one cycle but consumes power within the chip's thermal capacity for all other cycles. In this case, the circuit is not damaged, because the energy consumed—which corresponds to the peak power consumption time one cycle—will not be enough to elevate the temperature over

the chip's thermal capacity limit. To damage the chip, high power consumption must last for several cycles.

The scan-based design architecture are popular because of their low impact on performance and area. But these scan-based architecture are expensive because each test pattern requires a power-consuming shift operation to provide test patterns and evaluate test response. This phenomenon is well known in industry. To meet specified power limits during test and avoid system destruction, it is really important to reduce power dissipation during scan shifting.



Chapter 3

Power-driven Scan Cell Reordering

3.1 Previous Work

In this section, we introduce the previous work about scan cell reordering methodology to reduce power [20]. The prerequisite is the deterministic sets including test patterns and corresponding responses. The idea of the methodology is to find a scan cell ordering which generates the minimum transitions during shifting operation. (*scan – in* and *scan – out* operations)

The steps are described as following:

- Collect a deterministic sets of test patterns and corresponding responses.
- Determine a scan cell chaining to minimize total bit differences of adjacent cells in patterns and responses .
- Determine a scan cell ordering to minimize generated transitions during scan-in and scan-out operations.

The data in the first step is obtained from ATPG tool that generate the patterns with non-specified bits. In the second step, finding a scan cell chaining with the minimal

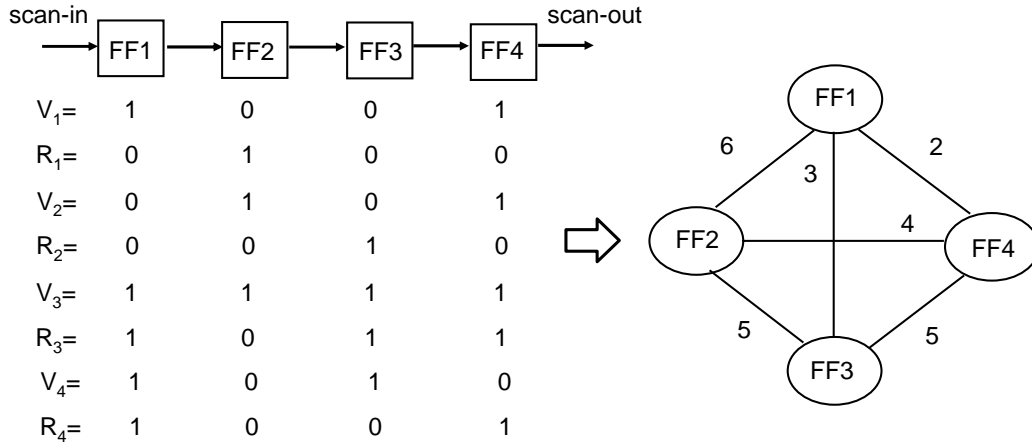


Figure 3.1: **Graph construction based on deterministic sets**

bit differences represents the high probability to minimize transitions as low as possible. A complete graph is constructed based on the deterministic sets to help us find out the solution. In the graph, a vertex denotes a scan cell and the edge weight represents the total bit difference of adjacent vertices. Figure 3.1 shows the graph construction based on deterministic sets. In the figure, the test sequence is composed of four test vectors (V_1 to V_4) and four output responses (R_1 to R_4). The scan chain has four flip-flops, hence scan vectors are four-bit long. The initial order of the scan cells in the scan chain is depicted on the figure. According to the above description, flip-flop 1, denoted FF1, corresponds to bit 1 in each scan vector, and so on.

Next, we calculate the total number of bit differences between each pair of scan flip-flops, which represents the number of transitions that may be generated in the corresponding portion of the scan chain by connecting these two flip-flops together. Calculating the total number of bit differences between each pair of flip-flops provides the following results: $d(\text{FF1}, \text{FF2}) = 6$, $d(\text{FF1}, \text{FF3}) = 3$, $d(\text{FF1}, \text{FF4}) = 2$, $d(\text{FF2}, \text{FF3}) = 5$, $d(\text{FF2}, \text{FF4}) = 4$, $d(\text{FF3}, \text{FF4}) = 5$.

To determine a scan cell chaining with the minimum cost, a greedy *traveling salesman problem* (TSP) is applied to find the solution. In the cases, the chaining of cells FF1-

FF4-FF2-FF3-FF1 is the final solution.

In the third step, the input and output of scan chain are identified. The transitions that bit differences generate during shift operation has dependency with its position of the scan chain. A novel method called *weighted transition counts* (WTC) had been proposed to calculate transitions [10].

Figure 3.2 shows different transition weight for test vectors and responses. For test vectors, the bit difference of cell pair close to scan chain output generates more transitions because of passing through a long path during scan-in operation. The transition weight is increasing from the scan chain input. On the contrary, the weight of out response is decreasing from the scan chain input. As a result, the various combinations of input and output of scan chains cause different transition counts.

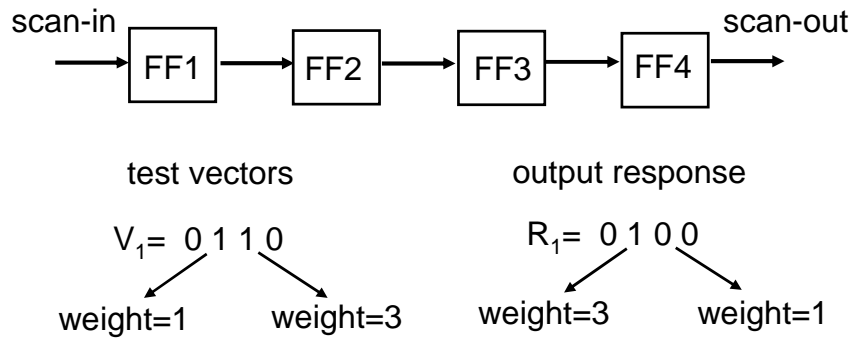


Figure 3.2: **Different transition weight for test vectors and responses**

The third step tries and calculates the weighted transition counts for different cases to find the best ordering of scan cells with the minimum generated transitions during shift operation. Figure 3.3 describes the operation. Taking the chaining FF1-FF4-FF2-FF3 for example, the value of WTC_{total} is derived by calculating the weighted transition counts of vectors and responses, respectively. Besides, the transitions generated due to the difference between the first bit of V_3 and the last bit of R_2 are also considered. The case FF1-FF4-FF2-FF3 has the minimum WTC_{total} and is the final ordering of scan

cells.

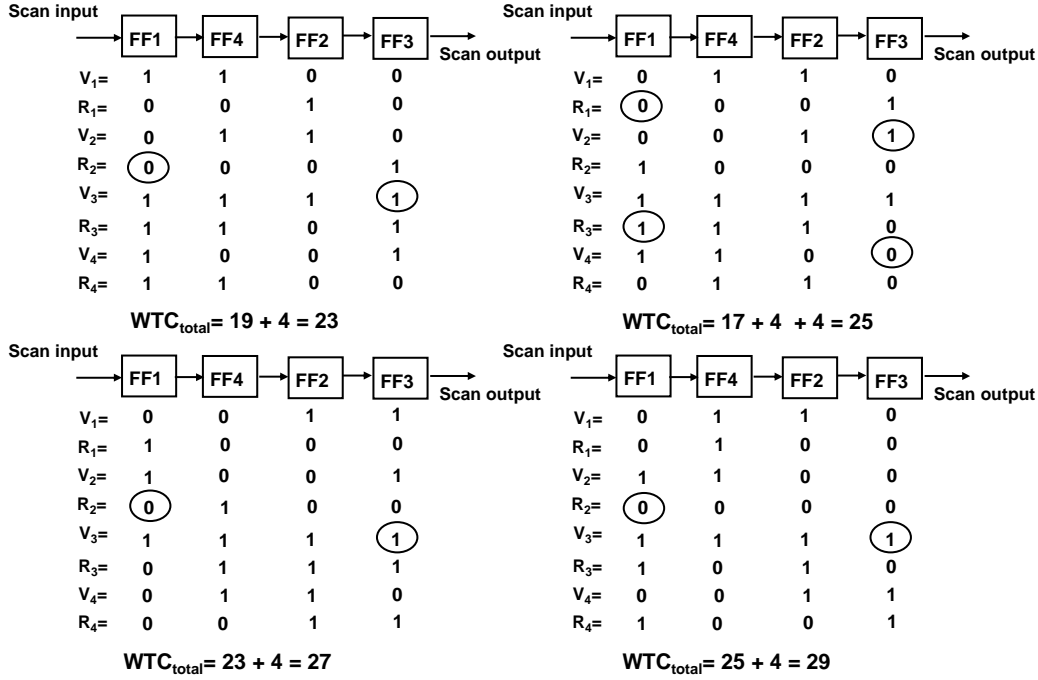
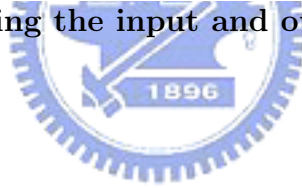


Figure 3.3: Identifying the input and output of scan chain



3.2 Motivation

During the scan-based testing, the total power consumption of the CUT is highly correlated with the total number of signal transitions on the scan cells [10]. In this thesis, we use the number of signal transitions on scan cells as the power model of the whole CUT. The proposed scan-cell-reordering scheme focuses on reducing the total scan-shift power, i.e., reducing the total scan-shift transitions. The capture power is not considered in the proposed scheme.

From the discussions in Chap. 1, the scan-in transitions can be minimized by wisely filling the don't-care bits of a test set once the scan-cell order in the scan paths are given [10]. This reduction could be more significant as the percentage of don't-care

bits increases. Therefore, our scan-cell reordering scheme attempts to first minimize the scan-out transition count without specifying the don't-care bits, leaving the don't-care bits for a later minimization of scan-in transition, such as MT-fill [10]. However, before specifying the don't-care bits, the value of some responses may not be obtainable, implying that no explicit information of scan-out transitions can be used during the scan-cell reordering process.

We use a simple experiment (reported in Table 3.1) to show that certain pairs of scan cells tend to have the same response value in most cases of the random don't-care filling. Thus the reordering scheme can avoid the possible scan-out transitions by connecting those correlated pairs of scan cells next to each other. We first define this tendency between two scan cells as the *response correlation*, which is the probability that the two scan cells have the same response value by a random fill of don't-care bits.

In the experiment, we use a commercial tool [26] to generate stuck-at-fault patterns with don't-care bits. We then collect the statistic of the response correlation between any two scan cells by randomly filling the don't-care bits and simulating the corresponding responses for 1-million times. Table 3.1 lists the range of response correlations (Columns 1 and 4), the number of scan-cell pairs whose sampled response correlation falls in the range (Columns 2 and 5), and its corresponding percentage to the total scan-cell pairs (Columns 3 and 6), for the largest ISCAS benchmark circuit s38584. As the results show, while majority of the scan-cell pairs have a response correlation around 0.5, still 21595 scan-cell pairs (2%) have a response correlation higher than 0.75. Those 21595 scan-cell pairs could form a fair-sized solution space when reordering the 1452 scan cells in s38584. This experimental result indicates that, even without specifying the don't-care bits, the response correlations are not purely random. The same trend can be observed on other ISCAS and ITC benchmark circuits as well.

Correlation	# of cell pairs	Distribution (%)	Correlation	# of cell pairs	Distribution (%)
0.95 - 1	32	0.003	0.45 - 0.50	476,539	45.220
0.90 - 0.95	758	0.072	0.40 - 0.45	34,963	3.319
0.85 - 0.90	2,549	0.242	0.35 - 0.40	12,957	1.230
0.80 - 0.85	6,531	0.620	0.30 - 0.35	9,260	0.879
0.75 - 0.80	11,725	1.113	0.25 - 0.30	6,910	0.656
0.70 - 0.75	17,097	1.623	0.20 - 0.25	5,109	0.485
0.65 - 0.70	17,518	1.663	0.15 - 0.20	3,666	0.348
0.60 - 0.65	21,848	2.074	0.10 - 0.15	1,949	0.185
0.55 - 0.60	46,804	4.443	0.05 - 0.10	748	0.071
0.50 - 0.55	376,600	35.750	0 - 0.05	0	0

Table 3.1: Response correlation of ISCAS benchmark s38584.

3.3 Problem Formulation

The problem of the scan-cell reordering for scan-shift power reduction is first defined as follows:

Input:

- A circuit under test with scan cells inserted, and
- ATPG test patterns with don't care bits (X's).

Output:

- An ordering of scan cells, and

- Test patterns with all don't-care bits specified by MT-Fill based on the derived cell ordering.

Objective:

- Generate the minimum number of scan-shift transitions for the given test patterns.

The proposed scan-cell-reordering scheme only discuss the situation of one scan chain in a design. However, the concept of the proposed reordering scheme could be extended to multiple-scan-chain architectures as well.

Given a test pattern and the scan-cell order for the scan chain, we can use the *weighted transition count* (WTC) [10] to calculate the number of scan-in and scan-out transitions. The WTC considers not only the value difference between the patterns or responses of two adjacent scan cells, but also the number of transitions that this value difference generates during the scan shift cycles. Equation 3.1 and 3.2 define the $WTC_{in}(i)$ and $WTC_{out}(i)$ to calculate the scan-in transitions and scan-out transitions generated by the i th pattern, respectively.

$$WTC_{in}(i) = \sum_{j=0}^{s-1} PD(j) \times W_{PD}(j) \quad (3.1)$$

$$WTC_{out}(i) = \sum_{j=0}^{s-1} RD(j) \times W_{RD}(j) \quad (3.2)$$

In equation 3.1 and 3.2, s denotes the total number of scan cells; $PD(j)$ ($RD(j)$) denotes the value difference between the scan-in pattern (scan-out response) of the j th cell and the $j + 1$ cell; $W_{PD}(j)$ denotes the number of scan-in transitions generated by the pattern-value difference $PD(j)$ when shifting in the corresponding pattern values from the scan input to the $j + 1$ cell; $W_{RD}(j)$ denotes the number of scan-out transitions generated by the response-value difference $RD(j)$ when shifting out the responses from the j cell to the scan chain output.

In the WTC calculation, $W_{PD}(j) = j$, implying that a pattern-value difference can generate more scan-in transitions if this value difference occurs closer to the scan-chain output. On the contrary, $W_{RD}(j) = s - 1 - j$, implying that a response-value difference can generate more scan-out transitions if this value difference occurs closer to the scan-chain input. Figure 3.4 shows an example of the WTC computation on a 6-cell scan chain, assuming that three value differences occur between cells (C_1, C_2) , (C_2, C_3) , and (C_5, C_6) for both the test pattern and its response.

Equation 3.3 calculates the total number of transitions, WTC_{total} , generated by a given test set with m test patterns.

$$WTC_{total} = \sum_{i=1}^m [WTC_{in}(i) + WTC_{out}(i)] \quad (3.3)$$

3.4 Scan-cell Reordering Considering Only Response Correlation



3.4.1 Detailed Steps of Reordering Scheme

We introduce a scan-cell reordering scheme, named *RORC* (ReOrdering considering Response Correlation), which first reduces the scan-out transitions by minimizing the response correlations while preserving all don't-care bits in the test patterns. Then, the scan-in transitions are further minimized by specifying the don't-care bits with MT-fill. Figure 3.5 shows the flow of RORC, which consists of five main steps. The detail of each step is described in the following subsections.

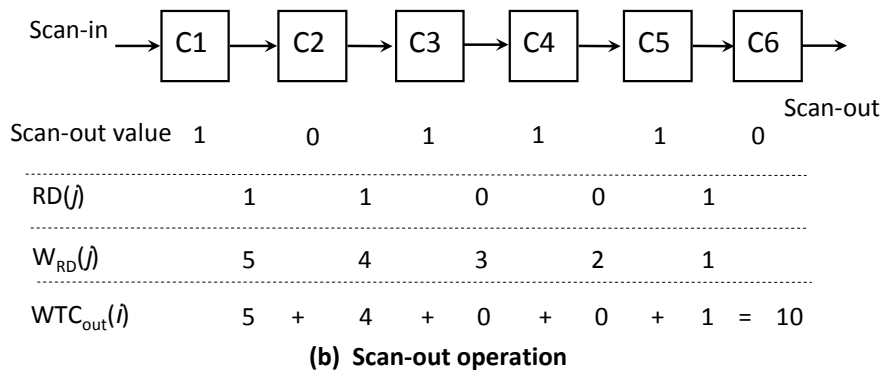
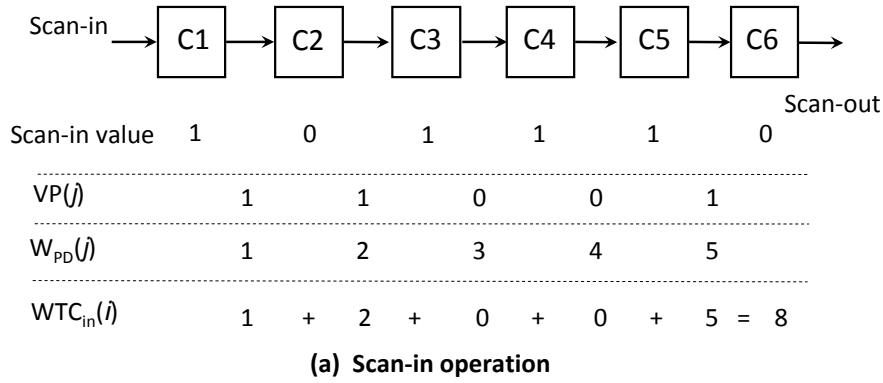



Figure 3.4: Calculation of scan-in and scan-out WTC.

Obtain Response Correlations

A simulation-based method is applied to sample the response correlations between each pair of scan cells. However, the filling of don't-care bits in RORC is not purely random since the MT-fill technique will be applied later in RORC. Therefore, in this step, we randomly generate the scan-cell ordering multiple times, specify don't-care bits using MT-fill based on each generated scan-cell ordering, and then collect the response correlations by simulating the filled patterns. The number of random-generated cell orderings used in simulation will determine the accuracy of the sampled response correlations. We use the following empirical equation to determine this number of random-generated cell

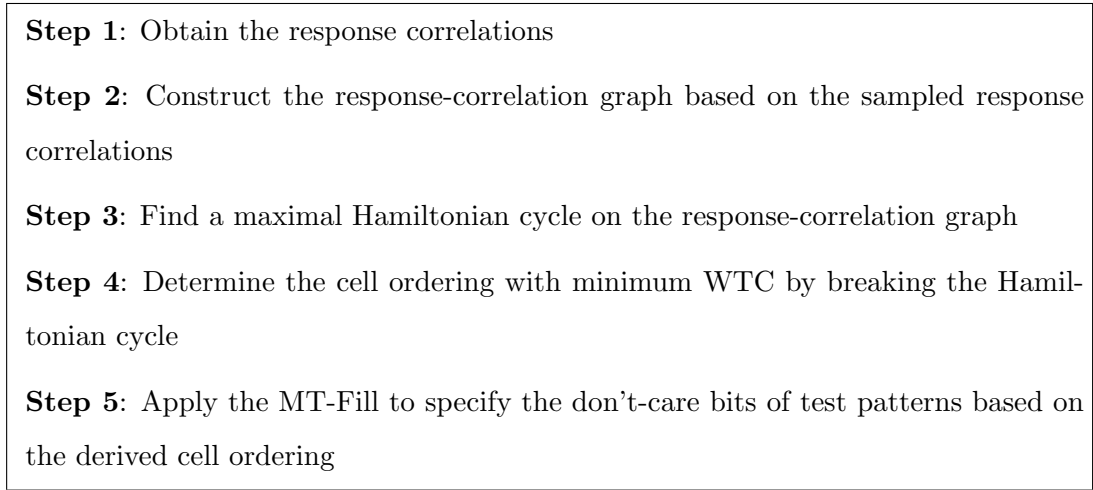
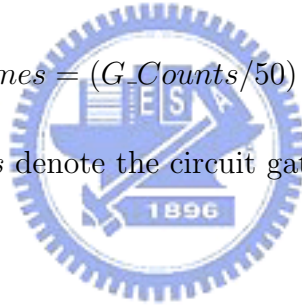


Figure 3.5: **Main steps of the proposed reordering scheme RORC.**

orderings.

$$Simulation_Times = (G_Counts/50) \times P_Counts, \quad (3.4)$$

where G_Counts and P_Counts denote the circuit gate count and the number of given test patterns, respectively.



Construct the Correlation Graph

After obtaining the response correlations, we construct a non-directed graph, named *response-correlation graph*, in which a vertex represents a scan cell and the weight of each edge represents the response correlation between the adjacent vertices. Because any pair of scan cells could be placed next to each other, the response-correlation graph is a complete graph. Figure 3.6 shows an example of constructing a response-correlation graph with four scan cells.

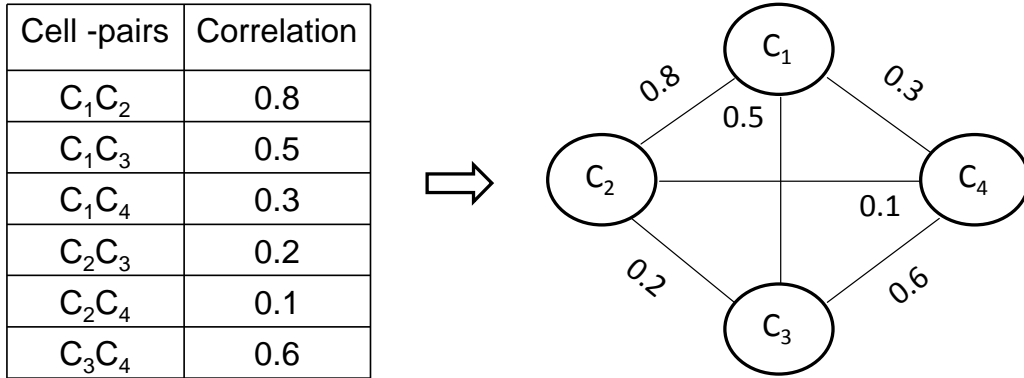


Figure 3.6: Construction of a response-correlation graph.

Find a Maximal Hamiltonian Cycle

A higher response correlation between two scan cells implies a lower probability that a response-value difference occurs between the two cells. Based on this concept, the maximum Hamiltonian cycle on the response-correlation graph implies a scan-cell ordering on which the number of value differences generated between adjacent cells is statistically minimum. Finding the maximum Hamiltonian cycle is known as the *traveling salesman problem* (TSP), which is NP-complete. We use a greedy TSP algorithm, which orders one vertex at a time to form the cycle. The selection criteria for the new ordered vertex is to find the vertex which has the maximum weight with the previous ordered vertex. In addition, we select the first N largest edges as the initial searching points and report the best result out of these N trials, where N denotes the total number of scan cells. The time complexity of this algorithm is $Q(N^3)$.

Determine Cell Ordering with Minimal WTC

In the previous step, we obtained a maximal Hamiltonian cycle on the response-correlation graph so that the number of potential response-value differences between adjacent cells can be minimized. However, to minimize the WTC_{out} , we need to con-

sider not only the number of response-value differences but also the positions of those value differences in the cell ordering (as discussed in Section 3.3). In Step 4, we break the given maximal Hamiltonian cycle into a Hamiltonian path, which forms the final scan-cell ordering. The breaking of the Hamiltonian cycle will affect the positions of the response-value differences and, in turn, affect the WTC_{out} . Here, we estimate the WTC_{out} generated by each possible breaking of the given Hamiltonian cycle and use the breaking with the minimum WTC_{out} to form the final cell ordering.

The estimated WTC_{out} here is obtained by replacing the $RD(j)$ in Equation 3.2 with 1 minus the response correlation between cell j and $j+1$. For example, the maximal Hamiltonian cycle in Figure 3.6 is $C_1-C_2-C_4-C_3-C_1$. Figure 3.7 shows the estimated WTC_{out} for all eight cases of the possible cycle breaking. The final cell ordering of the scan chain is $C_2-C_1-C_3-C_4$.

Apply MT-Fill to Specify Don't-care Bits

After the scan-cell ordering is decided in the previous step, we apply the MT-fill technique to fill the don't-care bits of the test patterns so that the scan-in transitions based on the scan-cell ordering can be minimized. The rule of MT-fill is that a don't-care bit is filled with the value of the first encountered specified bit when traversing from the don't-care bit toward the scan-chain output. Refer to [10] for more details of MT-fill.

3.4.2 Experimental Results

We conduct experiments on nine ISCAS and ITC benchmark circuits. Table 3.2 first shows the statistics of the benchmark circuits and their ATPG patterns generated by [26].

The following experiment compares RORC with another scan-cell reordering scheme presented in [20], which requires fully-specified test patterns before the reordering. Since RORC applies MT-fill to minimize the scan-in transitions, we apply MT-fill

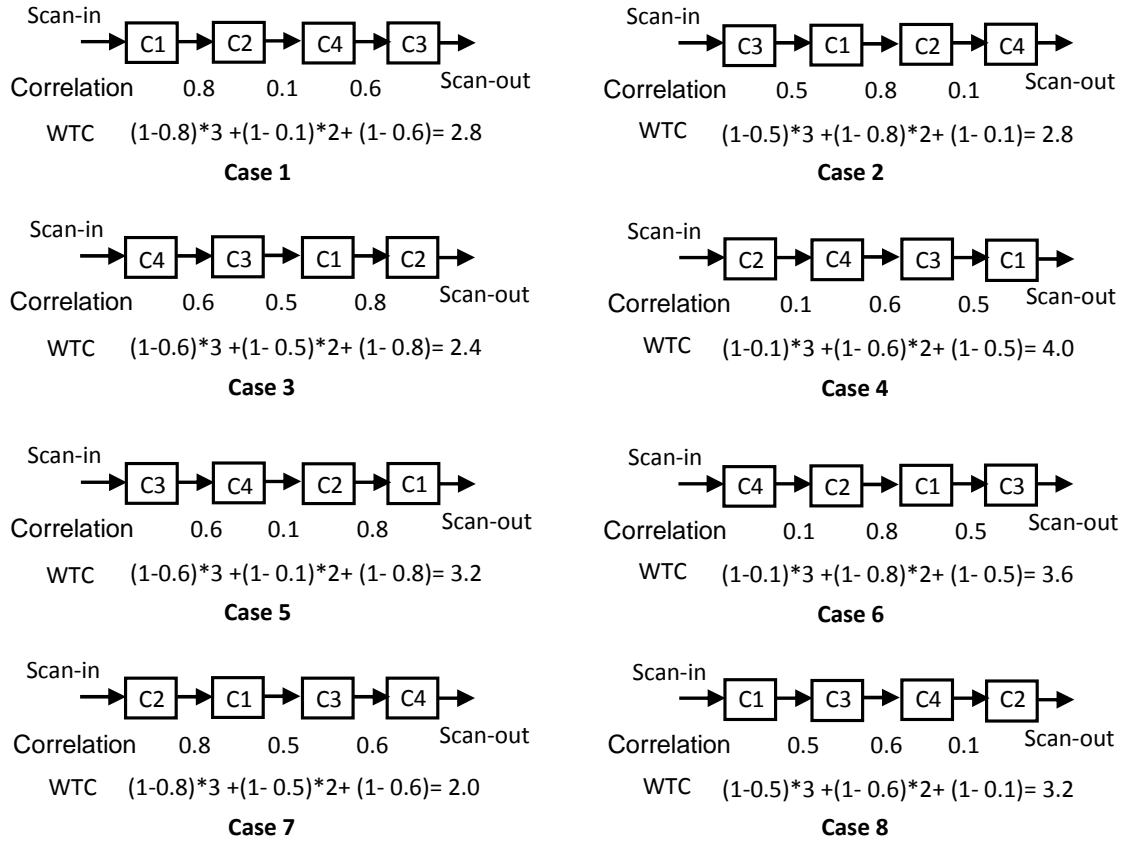


Figure 3.7: Estimated WTC_{out} of different scan-chain input/output.

for [20] as well. In the following experiment of [20], we first randomly generate an initial scan-cell ordering and specify the don't-care bits using MT-fill according to that initial ordering. Then the reordering scheme in [20] is applied to obtain the final scan-cell ordering based on the filled patterns. We repeat the above steps 100 times and report the best results for [20]. Also, we use the same TSP algorithm in both RORC and [20] to make a fair comparison.

In Table 3.3, Columns 3, 4, and 5 list the numbers of scan-in transitions, scan-out transitions, total scan-shift transitions, respectively. Column 6 lists the peak number of scan-shift transitions at a single scan-shift cycle. Column 7 lists the runtime in seconds. The results show that RORC can outperform [20] with an average 43.28%

circuit	gate count	PI	PO	# of scan cell	# of ATPG pattern	don't-care-bit percentage(%)	total faults	coverage (%)
s13207	7,951	31	121	669	108	79.65	21,190	100
s15850	9,772	14	87	597	117	75.35	23,244	100
s35932	16,065	35	320	1,728	24	37.36	57,084	100
s38417	15,106	28	106	1,636	167	78.94	61,754	100
s38584	19,253	12	278	1,452	148	78.01	71,278	100
b17	22,645	37	97	1,415	778	89.98	128,886	99.57
b20	8,875	32	22	490	539	73.37	47,040	99.56
b21	9,259	32	22	490	543	74.41	47,548	99.77
b22	14,282	32	22	735	530	75.51	70,750	99.91

Table 3.2: Statistics of the circuits and their ATPG patterns.

and 49.50% reduction to the number of scan-in transitions and scan-out transitions, respectively. The reduction to scan-in transitions first demonstrates the advantages of preserving don't-care bits for later minimization. Also, the reduction to scan-out transitions demonstrates the effectiveness of using sampled response correlations to guide the reordering process. The reduction to peak transitions is a byproduct of the reduction to total scan-shift transitions. Note that the result reported for [20] is selected from 100 trials of random initial cell ordering. It implies that, even with MT-fill, specifying all don't-care bits before reordering will significantly decrease the opportunity in minimizing scan-shift transitions later on and, in turn, lead to a local optimum.

RORC generates a lower number of total scan-shift transitions than [20] in all circuits but s35932. This exception may attribute to its low don't-care-bit percentage of 37.36%. From our internal experiments, we found that a cell ordering will affect the results of the MT-fill more significantly when the don't-care-bit percentage is lower. This finding further motivates us to develop a cell reordering scheme which can also consider the impact of a scan-cell ordering on the scan-in transitions generated by the

circuit	method	scan-in trans.	scan-out trans.	total trans.	peak trans.	runtime (sec)
s13207	[17]	3,951,373	4,188,819	8,140,192	289	400
	RORC	1,312,934	2,847,104	4,160,038	233	45
	improv.	66.77 %	32.03 %	48.90 %	19.38%	-
s15850	[17]	2,800,025	4,904,948	7,704,973	277	300
	RORC	1,497,065	2,157,662	3,654,727	211	49
	improv.	46.53 %	56.01%	52.57 %	23.83%	-
s35932	[17]	4,543,209	4,934,478	9,477,687	525	3,000
	RORC	5,388,270	4,363,125	9,751,395	680	120
	improv.	-18.60 %	11.58 %	-2.89 %	-29.52%	-
s38417	[17]	29,942,845	58,416,311	88,359,156	713	4,100
	RORC	11,453,864	27,547,170	39,001,034	529	666
	improv.	61.75 %	52.84 %	55.86 %	25.81%	-
s38584	[17]	22,827,002	41,743,137	64,570,139	714	3,100
	RORC	12,489,481	27,615,042	40,104,523	694	616
	improv.	45.29 %	33.85%	37.89 %	2.80%	-
b17	[17]	95,302,661	230,963,547	326,266,208	700	6,200
	RORC	24,619,742	41,550,664	66,170,406	570	3,760
	improv.	74.17 %	82.01%	79.72 %	18.57%	-
b20	[17]	7,680,415	12,332,467	20,012,882	237	500
	RORC	4,823,088	4,662,118	9,485,206	171	160
	improv.	37.20 %	62.20 %	52.60 %	27.85%	-
b21	[17]	7,351,208	11,834,023	19,185,231	229	600
	RORC	4,546,521	4,590,188	9,136,709	205	177
	improv.	38.15 %	61.21%	52.38 %	10.48%	-
b22	[17]	17,200,814	23,447,118	40,647,932	362	1,200
	RORC	9,997,996	10,844,186	20,842,182	276	587
	improv.	41.87 %	53.75 %	48.73 %	23.76%	-
Ave. improv.		43.68 %	49.50 %	47.30%	13.66%	-

Table 3.3: Comparisons of generated scan-shift transitions between RORC and [20].

MT-fill patterns.

3.5 Scan-cell Reordering Considering Both Response and Pattern Correlations

3.5.1 Detailed Steps of Reordering Scheme

RORC reduces scan-out transitions by minimizing the response correlations between adjacent cells. It ignores the impact of the cell ordering on the number of scan-in transitions resulted from the MT-fill patterns. In this section, we introduce another scan-cell reordering scheme, named *ROBPR* (ReOrdering considering Both Pattern and Response correlation), which can simultaneously optimize the pattern correlations and response correlations during the reordering process. Figure 3.8 shows the flow of ROBPR consisting of four main steps. The details of steps 1-3 are described in the following subsections. The detail of step 4 is the same as the step 5 in RORC and hence omitted in this section.

Step 1: Collect pattern and response correlations

Step 2: Construct a directed multiple-weight graph based on the collected pattern and response correlations

Step 3: Find the Hamiltonian path with the minimum WTC

Step 4: Apply the MT-Fill to specify the don't-care bits based on the derived cell ordering

Figure 3.8: Main steps of the proposed reordering scheme ROBPR.

Obtain Pattern and Response Correlations

In order to measure the impact of a scan-cell ordering on the number of scan-in transitions, we first define the *pattern correlation* between cell i and cell j as the probability that the pattern values on these two cells are the same when the output of cell i is connected to the input of cell j . Note that this pattern correlation is dependent on the order of cells. For a test pattern k , Table 3.4 considers each combination of pattern values between cell i and cell j , and lists its corresponding pattern correlation after MT-fill (denoted as $PC_k(i, j)$).

case	value of cell i	value of cell j	$PC_k(i, j)$
1	0	0	1
2	0	1	0
3	0	X	$S_0/(S_0 + S_1)$
4	1	0	0
5	1	1	1
6	1	X	$S_1/(S_0 + S_1)$
7	X	0	1
8	X	1	1
9	X	X	1

Table 3.4: **Different cases of pattern correlations between two adjacent cells.**

In cases 1, 2, 4, and 5, both values of cell i and j are specified bits and hence their pattern correlations can be determined immediately for test pattern k . In cases 7, 8, and 9, a don't-care bit are placed prior to a specified bit and hence the don't-care bit will be filled with the same value as the specified bit. In cases 3 and 6, a specified bit is placed prior to a don't-care bit. Hence, the value of this don't-care bit cannot be derived immediately and has to be determined by its first encountered specified bit when traversing toward the scan-chain output. We use $S_0/(S_0 + S_1)$ ($S_1/(S_0 + S_1)$) to represent the probability that its first encountered specified bit is a 0 (1), where S_0 and

S_1 denote the total numbers of specified 1s and 0s in the test pattern, respectively.

After calculating the $PC_k(i, j)$ for each pattern k , the pattern correlation between cell i and cell j for the entire test set can be obtained by averaging the $PC_k(i, j)$ for each pattern k .

As to the response correlations, we use the same simulation-based method described in the Sec. 3.4.1 to estimate them.

Construct the Directed Correlation Graph

The correlation graph constructed in ROBPR is a revised version of the correlation graph in Sec. 3.4.1. First, this correlation graph is directed. Second, an edge in this correlation graph has two weights (W_p, W_r) , where W_p and W_r represent the pattern correlation and response correlation, respectively. Figure 3.9 shows an example of constructing such a directed correlation graph given the pattern and response correlations between three scan cells.

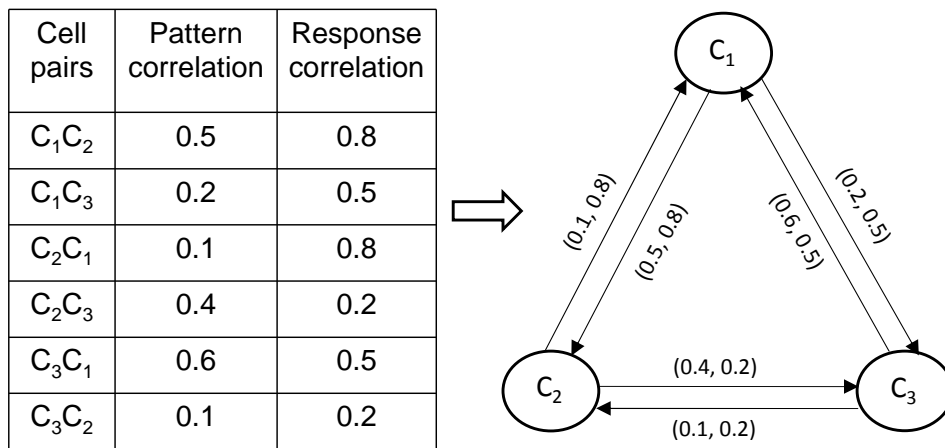


Figure 3.9: Construction of the directed graph based on pattern and response correlations.

Find the Hamiltonian Path with Minimal WTC

Unlike RORC which finds a Hamiltonian cycle first and then breaks the Hamiltonian cycle to obtain a Hamiltonian path with minimal estimated WTC_{out} , ROBPR uses an integrated algorithm to directly obtain the Hamiltonian path with minimal estimated WTC_{total} on the correlation graph. Figure 3.10 shows the proposed greedy-based algorithm, which also ordered one new vertex at a time to form such a Hamiltonian path.

When adding the n th non-ordered vertex V_{non} for the Hamiltonian path, this algorithm uses a cost function $Cost(V_{last}, V_{non}, n)$ to measure the impact of the new-added edge (V_{last}, V_{non}) on WTC_{total} , which is defined in Equation 3.3. In the definition of $Cost(V_i, V_j, n)$ in Figure 3.10, the $\overline{W}_p(V_i, V_j)$ ($\overline{W}_r(V_i, V_j)$) actually represents the probability that a pattern-value (response-value) difference occurs between V_i and V_j . The n in the cost function actually represents the $W_{PD}(n)$ described in the WTC equation 3.1. The $N - 1 - n$ in the cost function actually represents the $W_{RD}(n)$ described in the WTC equation 3.2.

This cost function will guide the algorithm to emphasize more on the response correlation in the beginning of the ordering process and then gradually move its emphasis to the pattern correlation in the later stage of the reordering process, which exactly reflects the WTC definition in Equations 3.1 and 3.2.

3.5.2 Experimental Results

We conduct experiments for ROBPR on the same benchmark circuits and test patterns as in Sec. 3.4.2. Table 3.5 compares the results of ROBPR with the results of RORC, which considers only the response correlation during the reordering. The experimental results show that, in average, ROBPR can generate 33.87% less scan-in transitions but only 5.01% more scan-out transitions compared to RORC. This signif-

```

1 #define
2    $W_p(V_i, V_j)$  : the pattern correlation of edge  $(V_i, V_j)$ 
3    $W_r(V_i, V_j)$  : the response correlation of edge  $(V_i, V_j)$ 
4    $\overline{W}_p(V_i, V_j) : 1 - W_p(V_i, V_j)$ 
5    $\overline{W}_r(V_i, V_j) : 1 - W_r(V_i, V_j)$ 
6    $Cost(V_i, V_j, n) : \overline{W}_p(V_i, V_j) \times n + \overline{W}_r(V_i, V_j) \times (N - 1 - n)$ 
7 begin
8    $N \leftarrow \#$  of cells ;  $n \leftarrow 1$  ;
9    $Min\_l \leftarrow$  a list of  $N$  edges having the minimum  $(\overline{W}_p + \overline{W}_r \times (N-1))$ ;
10  for each directed edge  $e(V_i, V_j)$  of  $Min\_l$ 
11     $V_{1st} \leftarrow V_i, V_{2nd} \leftarrow V_j, V_{last} \leftarrow V_{2nd}$ ;
12    while non-ordered  $V$ 
13       $cost_{min} \leftarrow \infty ; n \leftarrow (n + 1)$  ;
14      for each non-ordered  $V_{non}$ 
15        if  $(Cost(V_{last}, V_{non}, n) < cost_{min})$ 
16           $cost_{min} \leftarrow Cost(V_{last}, V_{non}, n)$  ;
17           $V_{next} \leftarrow V_{non}$  ;
18        endif
19      endfor
20       $V_{last} \leftarrow V_{next}$ 
21    endwhile
22  endfor
23 end

```

Figure 3.10: The proposed algorithm for finding a Hamiltonian path with minimal WTC_{total} .

icant reduction in scan-in transitions first demonstrates the advantage of adding the pattern correlations into consideration during the ordering process in ROBPR. It also shows the effectiveness of the pattern-correlation estimation listed in Table 3.4.

The average reduction to the total scan-shift transitions is 12.41% by ROBPR. The 8.05% reduction to the number of peak transitions is a byproduct of the reduction to total scan-shift transitions as well. The overall result again demonstrates the benefit of considering pattern correlations and response correlations simultaneously during the reordering. In addition, the reported runtime of ROBPR is almost the same as RORC, even though ROBPR needs to collect additional information for pattern-correlations calculation. It is because the proposed algorithm in ROBPR (Figure 3.10) can directly find the Hamiltonian path with minimal WTC_{total} , saving a step of breaking a Hamiltonian cycle to obtain the final ordering, such as Step 4 in RORC.

3.6 Scan-Cell Reordering Using Scan-data Inversion



3.6.1 Detailed Steps of Reordering Scheme

Both RORC and ROBPR utilize the high correlations to minimize the potential signal transitions since a high correlation between two cells represents a high probability that their response (or pattern) values are the same. On the contrary, a low correlation between two cells means that their response (or pattern) values are most likely inverse to each other. In this case, if we connect the inverse value of the cell (D') to the scan-in port (SI) of the other cell, the low correlation may be turned into a high correlation and become helpful for minimizing signal transitions. In this section, we introduce a scan-cell-reordering scheme, named SIRO (Scan-data-Inversion ReOrdering), which applies the scan-data-inversion technique and can take advantage of both high correlations and

circuit	method	scan-in trans.	scan-out trans.	total trans.	peak trans.	runtime (sec)
s13207	RORC	1,312,934	2,847,104	4,160,038	233	45
	ROBPR	882,926	2,780,763	3,663,689	168	45
	improv.	32.75 %	2.33 %	11.93 %	27.90%	-
s15850	RORC	1,497,065	2,157,662	3,654,727	211	49
	ROBPR	1,029,107	1,944,970	2,974,077	179	49
	improv.	31.26 %	9.86%	18.62 %	15.17%	-
s35932	RORC	5,388,270	4,363,125	9,751,395	680	120
	ROBPR	1,963,178	5,356,284	7,319,462	641	145
	improv.	63.57 %	-22.76%	24.94 %	5.74%	-
s38417	RORC	11,453,864	27,547,170	39,001,034	529	666
	ROBPR	9,599,399	29,676,522	39,275,921	521	667
	improv.	16.19 %	-7.73%	-0.70 %	1.51%	-
s38584	RORC	12,489,481	27,615,042	40,104,523	694	616
	ROBPR	10,064,216	27,385,766	37,449,982	580	618
	improv.	19.42%	0.83%	6.62 %	16.43%	-
b17	RORC	24,619,742	41,550,664	66,170,406	570	3,760
	ROBPR	16,202,102	46,655,210	62,857,312	563	3,765
	improv.	34.19 %	-12.29 %	5.01 %	1.23%	-
b20	RORC	4,823,088	4,662,118	9,485,206	171	160
	ROBPR	3,491,947	4,835,560	8,327,507	181	162
	improv.	27.60 %	-3.72 %	12.21 %	-5.85%	-
b21	RORC	4,546,521	4,590,188	9,136,709	205	177
	ROBPR	2,914,102	4,960,108	7,874,210	195	179
	improv.	35.90 %	-8.06 %	13.82 %	4.88%	-
b22	RORC	9,997,996	10,844,186	20,842,182	276	587
	ROBPR	5,603,864	11,233,009	16,836,873	261	588
	improv.	43.95 %	-3.59%	19.22 %	5.43%	-
Ave. improv.		33.87 %	-5.01 %	12.41 %	8.05%	-

Table 3.5: Comparisons of generated scan-shift transitions between RORC and ROBPR

low correlation between responses and patterns. Figure 3.11 shows the flow of SIRO consisting of four steps. The details of four steps are described as follows.

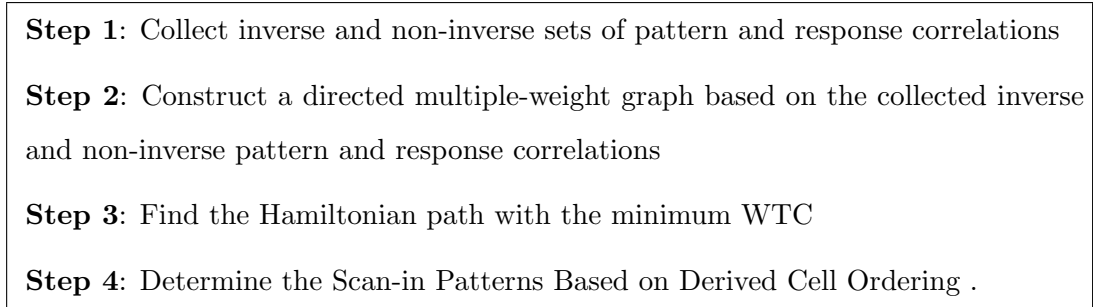


Figure 3.11: **Main steps of the proposed reordering scheme SIRO.**

Obtain Inverse Pattern and Response Correlations

In SIRO, when connecting a scan cell i to scan cell j , two types of connections can be made. One is direct connection, which connects D of i to SI of j , and the other is *inverse connection*, which connects D of i to SI of j . In RORC and ROBPR, we already discussed how to estimate the response and pattern correlations for the direct connection. The focus here is to estimate the response correlations and pattern correlations for the inverse connection.

The response correlation for an inverse connection can be simply estimated by 1 minus the response correlation calculated for a direct connection. However, the pattern correlations for an inverse connection are more complicated to estimate. This is because the MT-fill can adjust its filling of don't-care bits according to the inverse or direct connections. We first define the *inverse pattern correlation* between cell i and cell j for pattern k as $IPC_k(i, j)$, which is the probability that the pattern values on these two cells are the same when cell i is inversely connected to cell j . Table 3.6 shows the inverse pattern correlation for different combinations of pattern values between cell i and cell j after MT-fill. The derivation of Table 3.6 is similar to Table 3.4. The only

difference is that, for an inversely connected cell pair, a transition is generated when the specified values of both cells are "the same". The definition of S_0 and S_1 are the same as that in Table 3.4.

case	value of cell i	value of cell j	$IPC_k(i, j)$
1	0	0	0
2	0	1	1
3	0	X	$S_1/(S_0 + S_1)$
4	1	0	1
5	1	1	0
6	1	X	$S_0/(S_0 + S_1)$
7	X	0	1
8	X	1	1
9	X	X	1

Table 3.6: Different cases of inverse pattern correlations between two adjacent cells.

Construct the Directed Correlation Graph

The correlation graph constructed in SIRO is a revised version of the correlation graph in ROBPR. The difference is that an edge in this correlation graph has two sets of weights: non-inverse set (W_p, W_r) and inverse set (IW_p, IW_r), where W_p and W_r represent the direct pattern and response correlation as calculated in ROBPR, and IW_p and IW_r represent the inverse pattern correlation and response correlation as calculated in previous step. Figure 3.12 shows an example of constructing such a directed correlation graph given the inverse and non-inverse correlation sets between three scan cells.

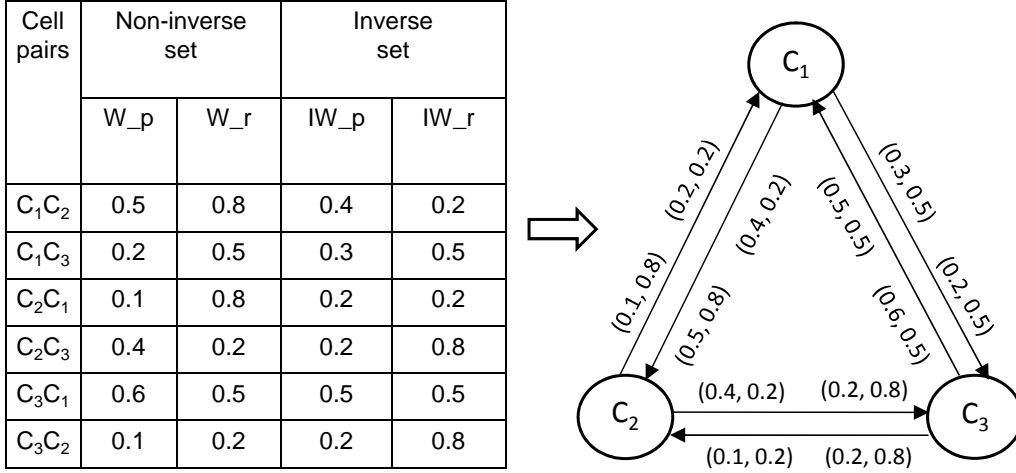


Figure 3.12: Construction of the directed graph based on inverse and non-inverse correlation sets.

Find the Hamiltonian Path with Minimal WTC

The algorithm in this step is similar to the algorithm in Figure 8, except two types of connections can be chosen in SIRO. When selecting to the n th ordered cell, SIRO needs to evaluate both the cost function for a direct connection $Cost(V_i, V_j, n)$ and the cost function for an inverse connection $Cost_{inv}(V_i, V_j, n)$. $Cost(V_i, V_j, n)$ is defined in ROBPR, and $Cost_{inv}(V_i, V_j, n)$ is defined as $IW_p(V_i, V_j) \times n + IW_r(V_i, V_j) \times (N - 1 - n)$. Therefore, the cell with the highest cost function is selected and the selected cell is connected accordingly to the type of the highest cost function ($Cost(V_i, V_j, n)$ or $Cost_{inv}(V_i, V_j, n)$).

Determine the Scan-in Patterns Based on Derived Cell Ordering

Unlike the RORC and ROBPR which directly use the traditional MT-fill to determine patterns based on the derived cell ordering, the MT-fill in SIRO needs to apply a different filling rule to handle inverse connections. First, the value of a specified bit is

inversed if an odd number of inverse connections are encountered before the specified bit. The specified bits remain the same if an even number of inverse connections are encountered. Next, the don't-care bits between the revised specified bits are filled using the traditional MT-Fill. Figure 3.13 shows an example of the revised MT-Fill to handle inverse connections.

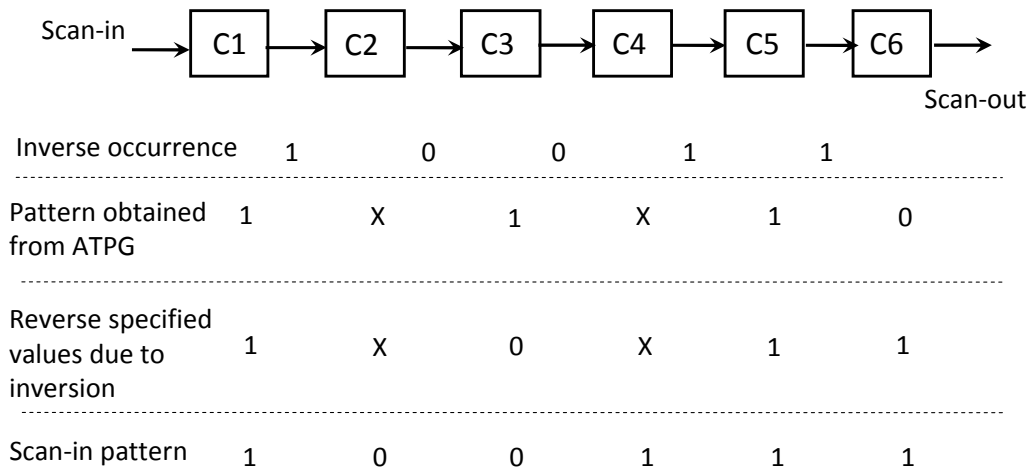


Figure 3.13: Derive scan-in patterns in SIRO .

In Figure 3.13, the scan chain contains six scan cells, and three inversions occur on cell pairs (C1,C2), (C4,C5), and (C5,C6), respectively. Because C2, C3, C4, and C6 pass through odd times of inversions (1 or 3 times) during scan-in operation, the specified values are inverted before MT-fill. Then the MT-fill is applied to fill all the don't-care bits according to the revised specified bits. Figure 3.14 shows the inverse connections of scan cells corresponding to the inverse occurrences of Figure 3.13. In Figure 3.14, the differences with traditional architecture is that \bar{Q} connects to SI while the inversions occur.

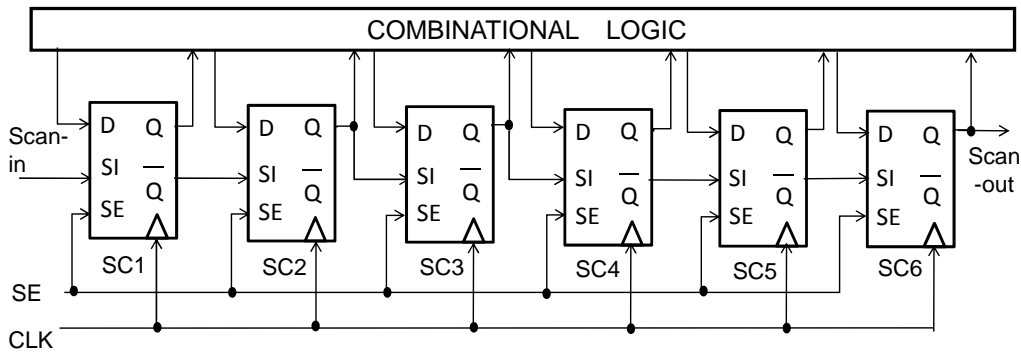


Figure 3.14: **Implement inverse techniques with traditional scan-chain architecture .**

3.6.2 Experimental Results

We conduct experiments for SIRO on the same benchmark circuits and test patterns as in Sec. 3.5.2. Table 3.7 compares the results of SIRO with the results of ROBPR, which considers only the non-inverse pattern and response correlation during the reordering. The results show that SIRO in average can generate 3.30% and -0.13% less scan-in and scan-out transitions, respectively. The reduction of scan-in transitions and slight increase in scan-out transitions explain limiting the number of inversions counts can reduce scan-in transitions under slightly affecting the accuracy of scan-out correlation.

The average improvement in total scan-shift transitions is 1.23%. Although the improvements of these experimental circuits are not significant, the overall result can improve as long as the inversions occur. Besides, the SIRO is dependent on circuit structure. For the circuits with the character of many low-correlation cell pairs, the SIRO is supposed to significantly reduce overall transitions. The reported runtime of SIRO is almost the same as ROBPR.


circuit	method	scan-in trans.	scan-out trans.	total trans.	peak trans.	runtime (sec)	inverse times
s13207	ROBPR	882,926	2,780,763	3,663,689	170	45	-
	SIRO	884,607	2,754,677	3,639,284	170	45	4
	improv.	-0.19 %	0.94 %	0.67 %	0.00	-	-
s15850	ROBPR	1,029,107	1,944,970	2,974,077	179	49	-
	SIRO	1,039,313	1,823,428	2,862,741	180	49	10
	improv.	-0.99 %	6.25 %	3.74 %	-0.56 %	-	-
s35932	ROBPR	1,963,178	5,356,284	7,319,462	641	145	-
	SIRO	1,963,178	5,356,284	7,319,462	642	145	0
	improv.	0 %	0 %	0 %	-	-	-
s38417	ROBPR	9,599,399	29,676,522	39,275,921	521	667	-
	SIRO	9,244,689	29,641,440	38,886,129	536	668	18
	improv.	3.70 %	0.12 %	0.99 %	-2.88 %	-	-
s38584	ROBPR	10,064,216	27,385,766	37,449,982	580	618	-
	SIRO	10,154,228	26,438,593	36,592,821	577	619	18
	improv.	-0.89 %	3.46 %	2.29 %	0.52 %	-	-
b17	ROBPR	16,202,102	46,655,210	62,857,312	563	3,765	-
	SIRO	16,202,102	46,655,210	62,857,312	563	3,768	0
	improv.	0.00 %	0.00 %	0.00 %	0.00 %	-	-
b20	ROBPR	3,491,947	4,835,560	8,327,507	181	162	-
	SIRO	3,095,170	5,103,108	8,198,278	176	162	2
	improv.	11.36 %	-5.53 %	1.55 %	2.76 %	-	-
b21	ROBPR	2,914,102	4,960,108	7,874,210	195	179	-
	SIRO	2,643,470	5,179,474	7,822,944	189	179	4
	improv.	9.29 %	-4.42 %	0.65 %	3.08 %	-	-
b22	ROBPR	5,603,864	11,233,009	16,836,873	261	588	-
	SIRO	5,188,530	11,457,397	16,645,927	259	589	8
	improv.	7.41 %	-2.00 %	1.13 %	0.77 %	-	-
Ave. improv.		3.30 %	-0.13 %	1.23 %	0.41%	-	-

Table 3.7: Comparisons of generated scan-shift transitions between ROBPR and SIRO

Chapter 4

Scan Cell Reordering Considering Both Power and Routing Factors

4.1 Detail Steps of Reordering Considering both Power and Routing Overhead



All above reordering schemes, such as RORC, ROBPR, and SIRO, focus on reducing the power consumption during scan-based testing. However, these reordering schemes may result in long wire length of scan paths because the connection of scan cells is determined by cells' response or pattern correlations, not cells' physical distance. In this section, we proposed a scan-cell reordering scheme, named ROPRO (ReOrdering considering Power and Routing Overhead), which combines the ROBPR with routing consideration. The same idea can be applied to SIRO as well.

In ROPRO, we reorder the scan cells after the placement is done. Based on the placement result, we use the manhattan distance between two scan cells to approximate the wire length. When selecting the next ordered scan cell, we incorporate this approximated wire length into the cost function and hence can limit the routing overhead.

In our implementation, the placement is done by a commercial back-end tool and the position of each scan cell is obtained by parsing its DEF file.

Basically, ROPRO contains almost the same five steps as that of ROBPR, except a modification to the step 2 and 3. Therefore, this subsection only shows the details of step 2 and 3. The rest steps all follow ROBPR.

4.1.1 Construct a Directed Multiple-Weight Graph Based on Correlations and Routing Overhead

As we said, the manhattan distance of cell pairs represent the routing overhead. To combine the routing overhead with correlation while constructing graph, the routing overhead is normalized between 0 to 1 by the difference of the longest and shortest manhattan distance of cell pairs.

The directed graph constructed in this section is a revised version combined the routing overhead with graph in ROBPR. An edge in the graph has three weights (W_p , W_r , W_l), where W_p , W_r and W_l represent the pattern correlation, response correlation, and routing weight, respectively. Figure 4.1 shows an example of constructing such a directed graph given the correlation and routing weight between three scan cells.

4.1.2 Find the Hamiltonian path with the minimum WTC

To control the tradeoff of ROPRO, we identify the cost function including both power and routing overhead. The cost function is defined as following:

$$C_T(V_i, V_j, \beta, n) = (1 - \beta) \times C_P(V_i, V_j, n) + \beta \times C_R(V_i, V_j) \quad (4.1)$$

where $C_P(V_i, V_j, n)$ represents the cost of power while reordering the n -th cell and $C_R(V_i, V_j)$ denotes the cost of routing. We can use the parameter β called *optimization factor* to adjust the optimization between power and routing. As the β increases, we

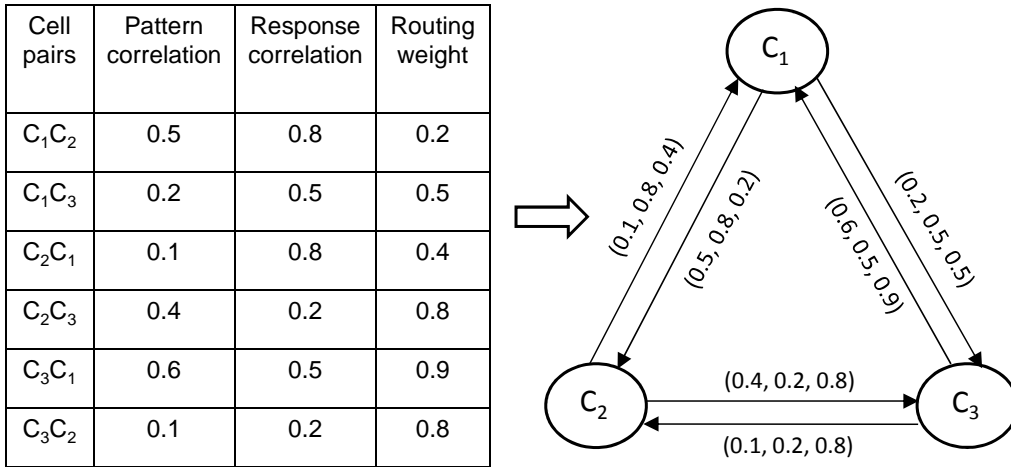


Figure 4.1: Construction of the directed graph based on correlations and routing effects.

make increasing effort on reducing routing length but the more power is generated. Here we use an integrated algorithm to find a Hamiltonian path with minimal cost $C_T(V_i, V_j, \beta, n)$ under specific β value. Figure 4.2 shows the proposed greedy-based algorithm, which also ordered one new vertex at a time to form such a Hamiltonian path.

When adding the n th non-ordered vertex V_{non} for the Hamiltonian path, we use the $C_T(V_i, V_j, n, \beta)$ to select the next cell. The $C_P(V_i, V_j, n)$ is similar to $Cost(V_i, V_j, n)$ described in Sec. 3.5.1 except it has to be normalized (divided by $(MaxCost - MinCost)$). As to routing cost, we use the similar method to normalize $C_R(V_i, V_j)$ (divided by $(MaxLength - MinLength)$), where $MaxLength$ and $MinLength$ represent the longest and shortest manhattan distance of cell pairs, respectively. The $C_T(V_i, V_j, n, \beta)$ guides the reordering algorithm to find a Hamiltonian path optimizing power and routing overhead under user-specific parameter β .

```

1  #define
2  Length( $V_i, V_j$ ) : length of edge( $V_i, V_j$ )
3  MaxCost : the maximum cost of  $Cost(V_i, V_j, n)$ 
4  MinCost : the minimum cost of  $Cost(V_i, V_j, n)$ 
5  MaxLength : the maximum length of edge( $V_i, V_j$ )
6  MinLength : the minimum length of edge( $V_i, V_j$ )
7   $C_P(V_i, V_j, n) : (Cost(V_i, V_j, n) - MinCost) / (MaxCost - MinCost)$ 
8   $C_R(V_i, V_j) : (Length(V_i, V_j) - MinLength) / (MaxLength - MinLength)$ 
9   $C_T(V_i, V_j, n, \beta) : (1 - \beta) \times C_P(V_i, V_j, n) + \beta \times C_R(V_i, V_j)$ 
10 begin
11   $N \leftarrow \#$  of cells ;  $n \leftarrow 1$  ;
12   $Min\_l \leftarrow$  a list of  $N$  edges having the minimum  $C_T(V_i, V_j, n, \beta)$ ;
13  for each directed edge  $e(V_i, V_j)$  of  $Min\_l$ 
14   $V_{1st} \leftarrow V_i, V_{2nd} \leftarrow V_j, V_{last} \leftarrow V_{2nd}$ ;
15  while non-ordered  $V$ 
16   $cost_{min} \leftarrow \infty$  ;  $n \leftarrow (n + 1)$  ;
17  for each non-ordered  $V_{non}$ 
18  if  $(C_T(V_{last}, V_{non}, n, \beta) < cost_{min})$ 
19   $cost_{min} \leftarrow C_T(V_{last}, V_{non}, n, \beta)$  ;
20   $V_{next} \leftarrow V_{non}$  ;
21  endif
22  endfor
23   $V_{last} \leftarrow V_{next}$ 
24  endwhile
25  endfor
26 end

```

Figure 4.2: The proposed algorithm for finding a Hamiltonian path optimizing power and routing overhead.

4.1.3 Experimental Results

We conduct experiments on the same benchmark circuits and test patterns as in 3.4.2, and all the comparisons of circuits are based on the same placements. Table 4.1 shows the total transitions on different optimization factor value and the comparisons with tool ordering result [27]. The result corresponding to β equaling to 0 is the same as the result of ROBPR in Sec3.5.2. Table 4.1 shows the power reduction corresponding to different optimization factor in ROPRO compared with tool result [27]. The results demonstrate the effectiveness of adjusting optimization factor and exhibit the trend that larger β value decrease the power reduction. The average reduction corresponding to β equaling to 0.0, 0.25, 0.5, and 0.75 are 53.71%, 52.55%, 50.36 %, and 46.42 %, respectively. (*ave improv.* represents $([27]-\text{ROPRO})/[27]$).

circuit	optimization factor value				Tool ordering [27]
	$\beta= 0.0$	$\beta= 0.25$	$\beta= 0.5$	$\beta=0.75$	
s13207	3,663,689	3,894,280	4,072,819	4,323,000	8,489,114
s15850	2,974,077	3,014,599	3,513,447	3,709,680	6,993,167
s35932	7,319,462	7,481,363	8,154,787	9,489,872	16,984,199
s38417	39,275,921	40,384,022	41,745,345	43,699,301	82,338,025
s38584	37,449,982	37,483,696	38,261,891	39,648,489	60,005,907
b17	62,857,312	64,606,969	68,303,575	83,978,396	294,941,487
b20	8,327,507	8,882,657	9,245,341	11,068,291	16,062,059
b21	7,874,210	9,156,139	9,370,271	10,127,148	174,034,433
b22	16,836,873	18,164,470	19,276,771	22,117,802	34,860,309
ave improv.	53.71 %	52.55%	50.36%	46.42%	-

Table 4.1: Comparisons of scan-shift transitions on different optimization factor value and tool ordering [27].

As to wire length of scan chain, we uses a TSMC 0.18gm CMOS technology with 5 metal layers to do the experiments. Table 4.2 shows the wire length of tool reordering

[27] compared with the different optimization factor in ROPRO. The reported length is obtained using commercial tool [27] after nanoroute. The results also demonstrate the scan chain length is minimized as the value of optimization factor increases. . Here the *ave improv.* represents the reduction percentage of tool ordering compared with ROPRO. ($(\text{ROPRO}-[27])/\text{ROPRO}$). The average reduction corresponding to β equaling to 0.0, 0.25, 0.5, and 0.75 are 78.90%, 65.99%, 56.05 %, and 37.99 %, respectively.

circuit	optimization factor value				Tool ordering [27]
	$\beta= 0.0$	$\beta= 0.25$	$\beta= 0.5$	$\beta=0.75$	
s13207	53,441	26,286	18,836	12,754	8,233
s15850	35,558	18,816	13,764	10,693	7,612
s35932	339,023	153,460	90,977	53,231	23,105
s38417	111,686	62,634	47,289	34,880	21,009
s38584	150,420	60,487	43,784	33,096	20,009
b17	70,797	52,774	42,844	36,552	22,372
b20	27,480	18,644	16,515	11,785	8,186
b21	29,588	19,576	14,820	12,040	7,857
b22	48,669	32,245	26,171	20,453	12,753
ave improv.	78.90 %	65.99 %	56.05 %	37.99 %	-

Table 4.2: Comparisons of scan chain length (um) on different optimization factor value and tool ordering [27].

Last, Figure 4.3 shows the trends of transitions and chain length by using broken-line-graph on the selected ISCAS and ITC circuits. (the biggest circuits) The line with triangle shapes represents the trend of transitions corresponding to different *optimization factor* β and tool ordering. In these figures, the trends demonstrate the effect of *optimization factor* β for each circuit. The transitions of each circuit increase with the increasing β and the chain length simultaneously decreases.

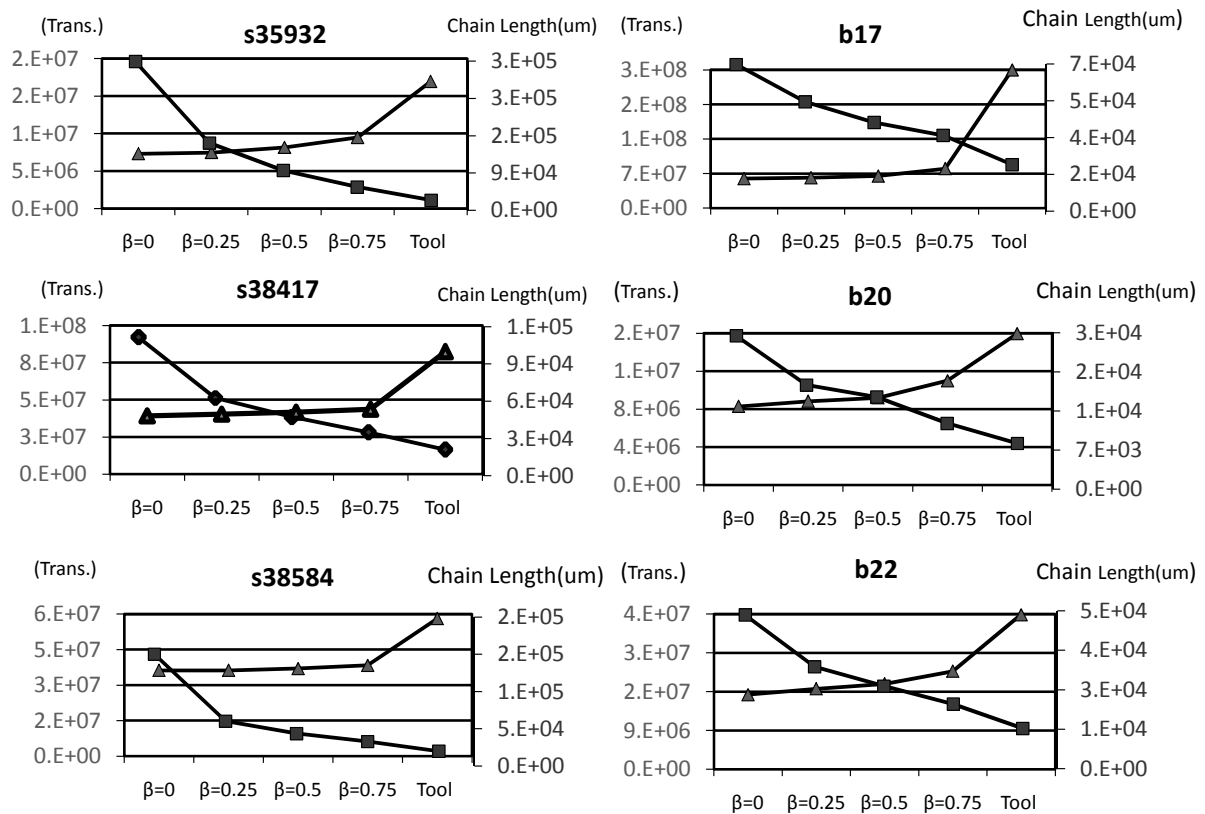


Figure 4.3: The trends of transitions and chain length on different constrain factor and tool ordering.

Chapter 5

Conclusions

This thesis first presents a scan-cell reordering scheme which connects the scan cells with a high response correlation to reduce scan-out transitions. This reordering scheme preserves the don't care bits during the ordering process so that a post pattern-filling technique can be applied to minimize the scan-in transitions. Next, a method that further adds the pattern correlations into consideration and reduce even more scan-shift transitions is given. Reverse technique can be applied to the ordering scheme to further reduce transitions. Last, a reordering scheme taking power and routing into consideration gives a tradeoff methodology of minimizing signal transitions and wire length. A set of experiments are conducted to demonstrated the effectiveness of each technique proposed in this thesis. A comparison to [20] also confirms the superiority to the scan-shift transitions.

The proposed schemes are assumed that one scan chain is used. The methodology for large designs may not be scalable because the huge CPU time to collect the correlation of scan cell pairs. To make the scheme more applicable, the scheme is required to extend to multiple scan chain architecture. The number of scan cells of each scan chain is reduced and thus the time collecting correlation decreases. The extension schemes about multiple scan chain are expected in the future work.

REFERENCES

- [1] M.L. Bushnell and V.D. Agrawal, "Essentials of Electronic Testing" , *Kluwer Academic Publishers* , ISBN 0-7923-7991-8, 2000.
- [2] Y. Zorian, "A distributed BIST control scheme for complex VLSI devices" , *Proc. 11th IEEE VTS*, pp.4-9, 1993
- [3] P. Girard, "Survey of Low-Power Testing of VLSI Circuits" , *IEEE Design C Test of Computers*, Vol. 19, No 3, pp.82-92, May-June 2002.
- [4] J. Saxena, K. M. Butler, V. B. Jayaram, S. Kundu, N. V. Arvind, P. Sreeprakash, and M. Hachinger, "A Case Study of IR-Drop in Structured At-Speed Testing" , *Proc. Intl. Test Conf.*, pp.1098-1104, 2003.
- [5] W. Li, S. M. Reddy, and I. Pomeranz, "On Reducing Peak Current and Power during Test" , *Proc. IEEE Comp. Society Annual Symp. On VLSI*, pp. 156-161, 2005.
- [6] S. Remersaro, X. Lin, Z. Zhang, S.M. Reddy, I. Pomeranz, and J. Rajski, "Preferred fill: a scalable method to reduce capture power for scan based designs" , *Proc. Int. Test Conf.*, paper 32.2, 2006
- [7] X. Wen, Y. Yamashitam, S. Kajihara, Kajihara, L. T. Wang, K. K. Saluja, and K. Kinoshita, "On Low-Capture-Power Test Generaion for Scan Testing" , *Proc. VTS*, pp. 265-270, 2005
- [8] R. Sankaralingam and N. A. Touba, "Controlling peak power during scan testing" , *Proc. VTS*, pp. 153-159, 2002.
- [9] X. Wen, S. Kajihara, K. Miyase, T. Suzuki, K. Saluja, L.-T. Wang, K. Abdel-Hafez, and K. Kinoshita, "A New ATPG Method for Efficient Capture Power Reduction During Scan Testing" , *Proc. VLSI Test Symp.*, pp. 58-63, 2006.
- [10] R. Sankaralingam, R. R. Oruganti, and N. A. Touba, "Static compaction techniques to control scan vector power dissipation" , *Proc. VTS*, pp. 35-40, 2000

- [11] G. Mrugalski, J. Rajska, D. Czysz and J. Tyszer, "New Test Data Decompressor for Low Power Applications" , *Proc. DAC*, pp. 539-544, 2007
- [12] SP Lin, CL Lee, JE Chen, JJ Chen, KL Luo, and WC Wu, "A Multilayer Data Copy Scheme for Low Cost Test with Controlled Scan-In Power for Multiple Scan Chain Designs" , *Int. Test Conf.*, 2006
- [13] O. Sinanoglu and A. Orailoglu, "Modeling Scan Chain Modifications for Scan-in Test Power Minimization" , *Int. Test Conf.*, 2003.
- [14] Y. Bonhomme et al., "A Gated Clock Scheme for Low Power Scan Testing of Logic ICs or Embedded Cores" , *Proc. 10th Asian Test Symp. (ATS 01)*, IEEE CS Press, Los Alamitos, Calif. pp. 253-258, 2001
- [15] P. Rosinger, B.M. Al-Hashimi, and N. Nicolici, "Scan Architecture With Mutually Exclusive Scan Segment Activation for Shiftand Capture-Power Reduction" , *IEEE Transactions on Computer-Aided Design (TCAD)*, Vol. 23 , No. 7, pp. 1142-1153, July 2004
- [16] L. Whetsel, "Adapting Scan Architectures for Low Power Operation" , *Proc. IEEE Int. Test Conf.* , pp. 863-872, 2000
- [17] J. Saxena, K. M. Butler, and L. Whetsel, "An analysis of power reduction techniques in scan testing" , *Proc. IEEE Int. Test Conf.*, pp. 670-677, 2001
- [18] T.-C. Huang and K.-J. Lee, "A token scan architecture for low power testing" , *Proc. Int. Test Conf.*, pp. 660-669, 2001.
- [19] R. Sankaralingam, B. Pouya, and N.A. Touba, "Reducing power dissipation during test using scan chain disable" , *Proc. 19th VLSI Test Symp. (VTS 01)*, IEEE CS Press, Los Alamitos, Calif., pp. 319-324, 2001
- [20] Y. Bonhomme, P. Girard, L. Guiller, C. Landrault, and S. Pravossoudovitch, "Power driven chaining of flip-flops in scan architectures" , *Int. Test Conf.*, pp. 796-803, 2002.
- [21] V. Dabholkar, S. Chakravarty, I. Pomeranz, and S. Reddy, "Techniques for reducing power dissipation during test application in full scan circuits" , *IEEE Transactions on CAD*, 17(12):1325V 1333, December 1998.

- [22] S Makar, “A layout-based approach for ordering scan chain flip-flops” , *Proc. of the IEEE Int. Test Conf.*, pp. 341-347, 1998.
- [23] M Hirech, J Beausang, and X Gu, “A New Approach to Scan Chain Reordering Using Physical Design Information” , *IEEE Int. Test Conf.* ,pp. 348-355, 1998.
- [24] Y. Bonhomme, P. Girard, L. Guiller, C. Landrault, and S. Pravossoudovitch, “Efficient Scan Chain Design for Power Minimization During Scan Testing Under Routing Constraint” , *IEEE Int. Test Conf.*, pp. 488-493, 2003.
- [25] Y. Bonhomme, P. Girard, L. Guiller, C. Landrault, S. Pravossoudovitch, A. Virazel, “Design of routing-constrained low power scan chains” , *Proc. DATE*, pp. 62-67, 2004
- [26] Synopsys TetraMAX ATPG User Guide Version X-2005.09
- [27] Cadence Encounter Product Version 5.2.3 June 2006



學經歷

姓 名：吳育澤

性 別：男

籍 貫：臺南縣

出生日期：民國七十二年二月十三日

通訊地址：台南縣新營市新北八街 53 號 6 樓之一，電話：(06)6591557

學經歷：民國九十四年九月至民國九十七年一月
 國立交通大學電子研究所碩士班
 民國九十年九月至民國九十四年六月
 國立中央大學電機工程學系

論文題目：掃描鏈重新排列減少掃描移動功率架構在非指定的測試集合

Scan-Chain Reordering for Minimizing Scan-Shift Power
Based on Non-Specified Test Cubes